Supporting Information for

Opposite Thermal Expansion in Isostructural Non-collinear Antiferromagnetic Compounds of Mn_3A (A = Ge and Sn)

Yuzhu Song[†,‡], Yongqiang Qiao[‡], Qingzhen Huang[§], Chinwei Wang[‖], Xinzhi Liu[⊥], Qiang Li[‡], Jun Chen[†,‡,*] and Xianran Xing[†,‡]

[†] Beijing Advanced Innovation Center for Materials Genome Engineering, University of Science and Technology Beijing, Beijing 100083, China

[‡] Department of Physical Chemistry, University of Science and Technology Beijing, Beijing 100083, China

[§] NIST Center for Neutron Research, National Institute of Standards and Technology, Gaithersburg MD, 20899-6102, USA

[‖] Neutron Group, National Synchrotron Radiation Research Center, Hsinchu 30077, Taiwan

[⊥] Helmholtz-Zentrum-Berlin für Materialien und Energie, Hahn-Meitner-Platz 1, D-14109 Berlin, Germany

*Corresponding author: junchen@ustb.edu.cn

1. **Sample preparation:** The samples of polycrystalline of Mn_3Ge were prepared using precursor elements with better than 99.9% purity via arc melting under a high-purity argon atmosphere. To ensure homogeneity, the button samples were turned over and melted many times. After melting, the samples were wrapped with Mo foils, then annealed in a vacuum-sealed quartz tube at 1073 K for 6 days and subsequently quenched in water.

2. **Experiment methods:** The linear thermal expansion ($\Delta l/l_0$) was measured using a thermodilatometer (DIL 402 Expedis Select). Temperature dependence of high-intensity NPD data with λ = 2.41 Å were collected at the high-intensity diffractometer Wombat of the Australian Nuclear Science and Technology Organisation (ANSTO). Temperature dependence of the usual NPD data was collected using the BT-1 neutron powder diffractometer at the NIST Center for Neutron Research. The wavelength of the neutron beam was 1.5397 Å. The high-intensity synchrotron X-ray diffraction patterns of $Mn_3(Ge_{1-x}Sn_x)$ at room temperature were collected at the beamline 11-ID-C of APS, Argonne National Laboratory with high-energy X-ray radiation (λ= 0.1173 Å). The magnetism properties were measured using the Quantum Design physical property measurement system (PPMS) with the vibrating sample magnetometer (VSM). The mechanical properties of Mn_3Ge ingots with a diameter of 2 mm and a length of 5 mm were obtained using a mechanical testing machine (Instron-5966) at room temperature. The electrical conductivity and thermal conductivity properties were measured using a standard four-probe method and a steady-state method,

respectively. The structural refinements for all NPD data were analysed using the FULLPROF software.

3. Supplementary Figures

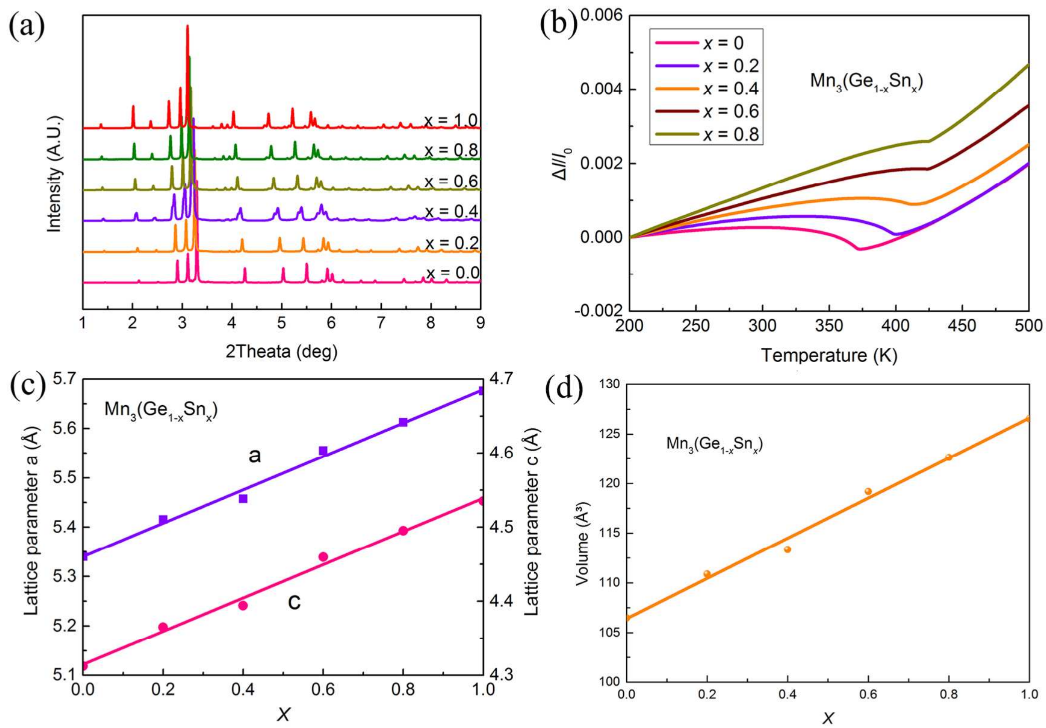

Figure S1. Crystal structure and thermal expansion property of $Mn_3(Ge_{1-x}Sn_x)$ (x = 0, 0.2, 0.4, 0.6, 0.8, 1.0). (a) High-intensity SXRD patterns of $Mn_3(Ge_{1-x}Sn_x)$ at room temperature. (b) Linear thermal expansion property of $Mn_3(Ge_{1-x}Sn_x)$ determined by a dilatometer. (c) Lattice parameters *a* and *c* of $Mn_3(Ge_{1-x}Sn_x)$ as function of *x*. (d) Unit cell volume of $Mn_3(Ge_{1-x}Sn_x)$ as function of *x*.

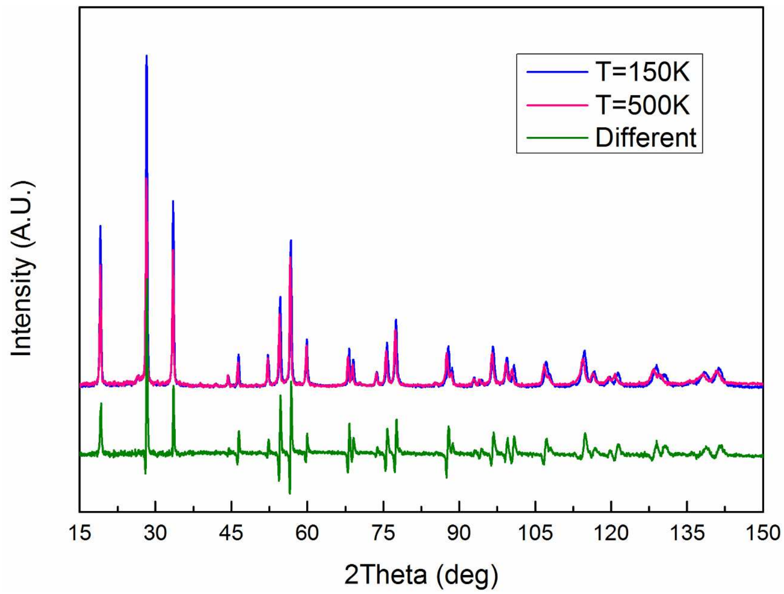

Figure S2. The NPD patterns of Mn_3Ge at different temperature (T = 150 K and T = 500 K). The difference at the bottom represents the contribution of the magnetic structure to the diffraction peaks.

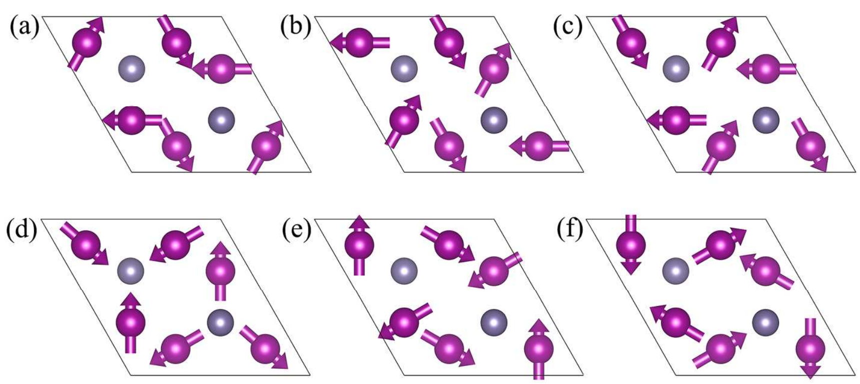

Figure S3. Triangular antiferromagnetic structural models. The possible triangular antiferromagnetic structural models allowed by the symmetry of $P6_3/mmc$ structure and its subgroups.

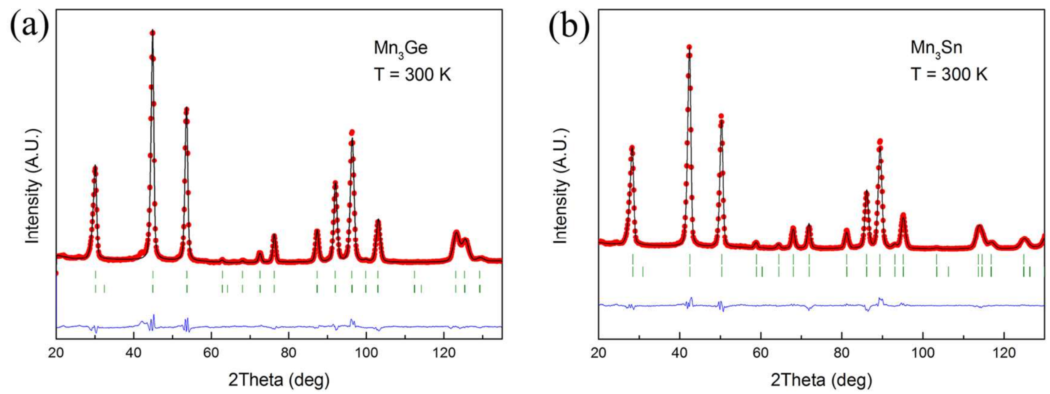

Figure S4. Structure refinements of high-intensity NPD patterns of (a) Mn_3Ge, and (b) Mn_3Sn at T = 300 K. The propagation vector of magnetic structure is $\boldsymbol{k}$ = (0, 0, 0), since no additional peaks and only the additional contribution to the nuclear peaks can be observed.

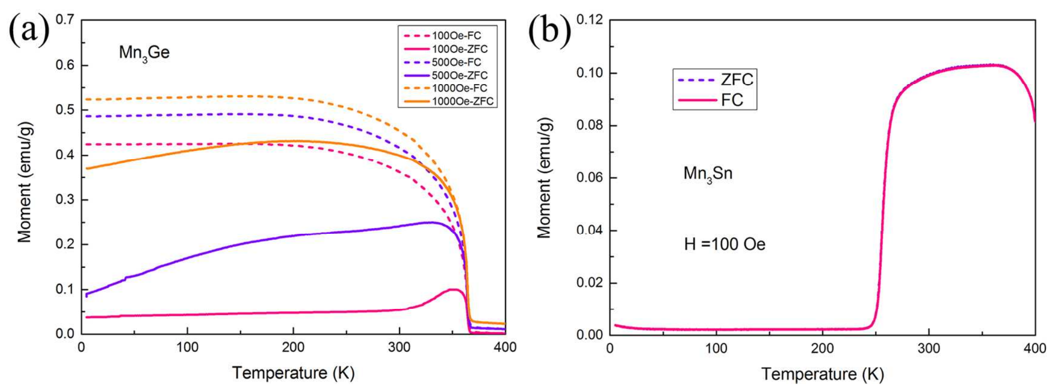

Figure S5. Macroscopic magnetic behavior of Mn_3Ge and Mn_3Sn. Temperature dependences of zero-field-cooling (ZFC) and field-cooling (FC) magnetization under different magnetic fields for the (a) NTE Mn_3Ge and (b) PTE Mn_3Sn.

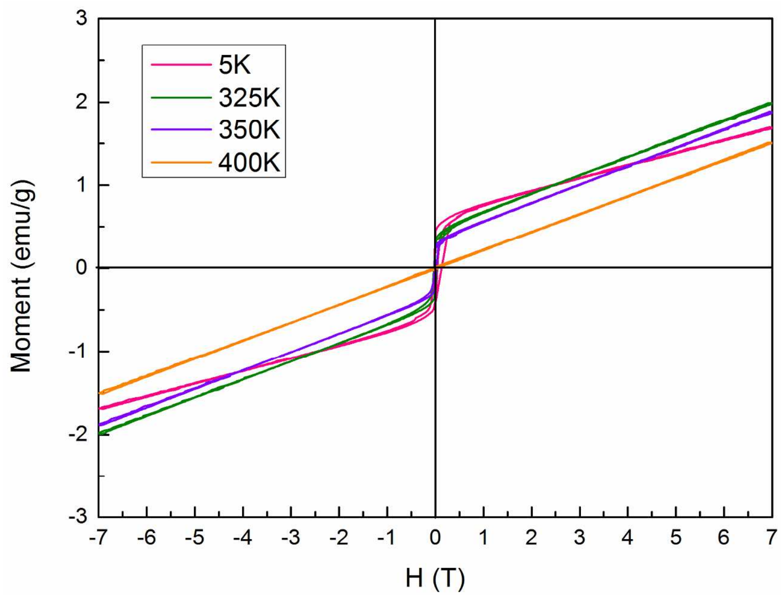

Figure S6. *M-H* curves for Mn_3Ge. Isothermal magnetization curves measured at T = 5, 325, 350, 400 K.

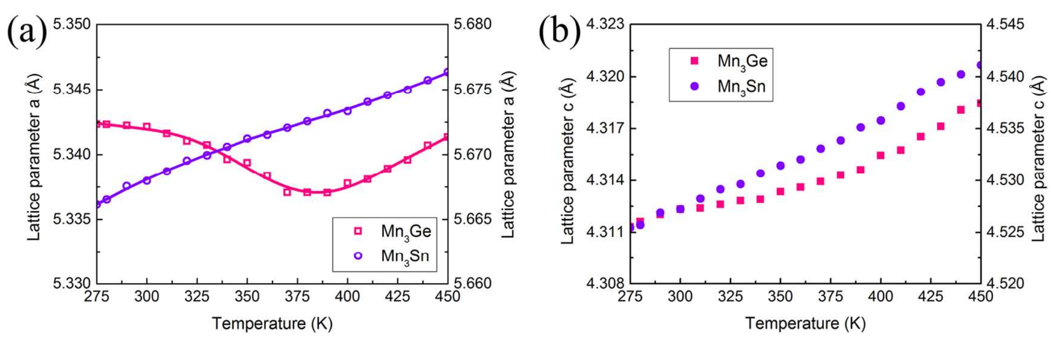

Figure S7. Temperature dependence of lattice parameters (a) *a* and (b) *c* for Mn_3Ge and Mn_3Sn.

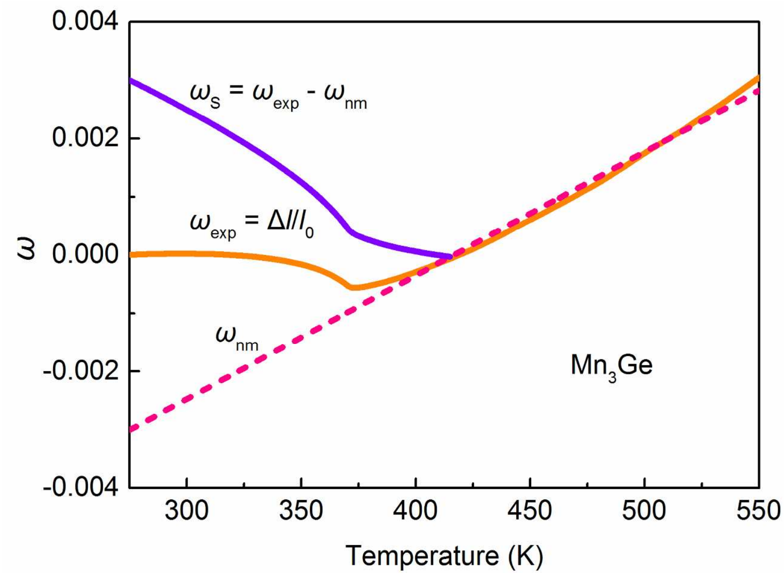

Figure S8. Thermal expansion properties of Mn_3Ge. ω_{exp} is experimental linear thermal expansion data measured by thermo-dilatometer, ω_{nm} is the nominal thermal expansion contributed from the nonmagnetic state, which is calculated according to the Debye-Grüneisen relationship, and ω_s ($\omega_s = \omega_{exp} - \omega_{nm}$) is the contribution of spontaneous volume magnetostriction from magnetic ordering.

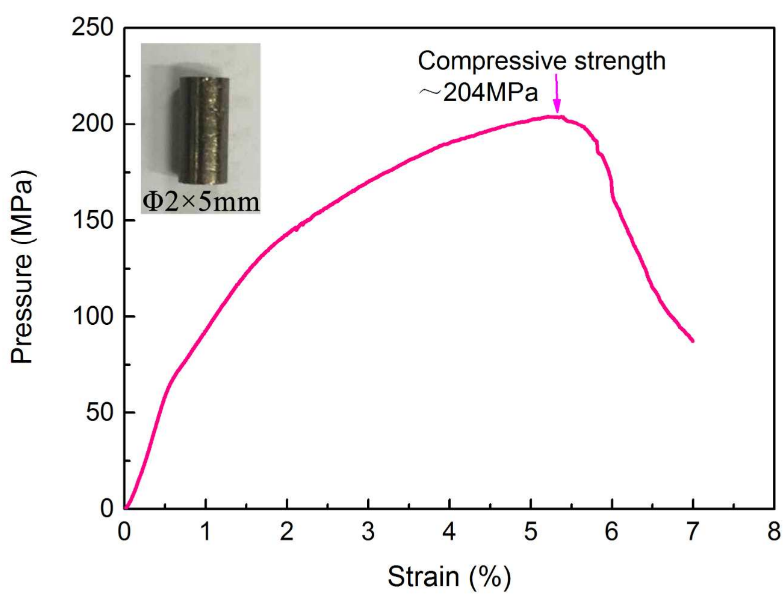

Figure S9. Mechanical properties of the NTE Mn_3Ge sample. The engineering stress–strain curve of the Mn_3Ge ingots at room temperature.

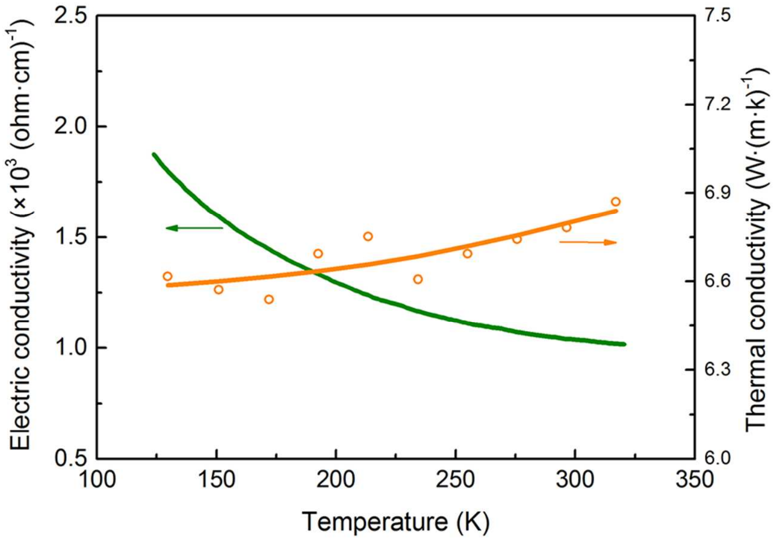

Figure S10. Temperature dependence of the electrical and thermal conductivity properties.